Faculty of Science

CHARACTERIZATION OF THE ANTIMICROBIAL SECONDARY METABOLITES PRODUCED BY THE CAVE-DWELLING *STREPTOMYCES* SP. ICC1 STRAIN

2019 | ALYSHA EILEEN MILWARD

B.Sc. Honours thesis – Chemical Biology

THOMPSON RIVERS UNIVERSITY

CHARACTERIZATION OF THE ANTIMICROBIAL SECONDARY METABOLITES PRODUCED BY THE CAVE-DWELLING *STREPTOMYCES* SP. ICC1 STRAIN

by

ALYSHA EILEEN MILWARD

A THESIS SUBMITTED IN PARTIAL FULFILLMENT
OF THE REQUIREMENTS FOR THE DEGREE OF

BACHELOR OF SCIENCE (HONS.)
in the
DEPARTMENTS OF BIOLOGICAL SCIENCES
AND PHYSICAL SCIENCES
(Chemical Biology)

This thesis has been accepted as conforming to the required standards by:
Dr. Heidi Huttunen-Hennelly (Ph.D.), Thesis Supervisor, Dept. Physical Sciences
Dr. Naowarat Cheeptham (Ph.D.), Co-Supervisor, Dept. Biological Sciences
Dr. Kingsley Donkor (Ph.D.), External Examiner, Dept. Physical Sciences

Dated this 30th day of April, 2019, in Kamloops, British Columbia, Canada

ABSTRACT

The desolate environment of the Iron Curtain Cave in Chilliwack, British Columbia, houses the *Streptomyces* sp. ICC1 strain shown to secrete antimicrobial secondary metabolite(s). Effective against both laboratory and multi-drug resistant strains of *Escherichia coli* and *Staphylococcus aureus*, the bioactivity has been thought to arise from the resilient physiology and specialized metabolic pathways that are known to exist within extreme-condition microbial species. Following optimization methods through liquid organic solvent extractions and both analytical and preparative reversed-phase high performance liquid chromatography techniques, the bioactive secondary metabolite(s) have been reasoned to exhibit both polar and non-polar substituents. Continued structural elucidation via one-dimensional proton nuclear magnetic spectroscopy suggested an unlikely peptidic nature to the antimicrobial compound(s) produced by the cave-dwelling *Streptomyces* sp. ICC1 strain. Therefore, further instrumental analysis on pure samples must be performed to reveal the true molecular nature of the bioactive metabolite(s), as well as mode-of-action analyses.

Thesis Supervisor: Heidi Huttunen-Hennelly, Ph.D.

ACKNOWLEDGEMENTS

I would like to express my sincere gratitude to my supervisor Dr. Heidi Huttunen-Hennelly for her continuous support and knowledge, but also her motivation and patience through the inescapable pitfalls. To Dr. Naowarat Cheeptham for access to her laboratory and its resources and for her perception and immense understanding of life at the microscopic level. To Trent Hammer for his unwavering assistance and navigation through instrumental set-up and analysis. To Arjun Banskota for preliminary NMR analysis through correspondence with the National Research Council, Canada. Further, to Dr. Kingsley Donkor for his contributions as external examiner and for his analytical expertise.

TABLE OF CONTENTS

LIST OF FIGURES

LIST OF TABLES

INTRODUCTION

The uprising of drug-resistant microbes has been a compounding event since the first observed bacterial resistance from a strain of *Staphylococcus* against the revolutionary discovery of penicillin in 1928. To date, antibiotic resistance was commonly misconceived to be the result of human misuse. Although undoubtedly a strong contributor, one study of note found that the antibiotic resistome in a bacterium from the Lechuguilla Cave, New Mexico, pre-dates the use of antibiotics by humans (Bhullar *et al*. 2012). In such a way, antibiotic resistance can be thought to be an entirely natural occurrence in bacterial evolution, that may have only be expedited by human interaction. Currently, antimicrobial resistance has been the cause of death of an estimated 700,000 individuals each year—predicted by the World Health Organization to reach 10 million by 2050 (Sarkar *et al*. 2017). The demand for alternatives to currently available pharmaceuticals continually increases as evolution of both man and bacterial species inevitably progresses.

Distinguishing Gram-Positive and Gram-Negative Bacteria

Although diverse, bacterial species exist in either one of two categories: Gram-positive or Gram-negative. The cell wall, common to all bacterial species (*Mycoplasma* exempt), differs in structure and chemical composition between Gram-positive and Gram-negative bacteria. Primarily, the thickness of the peptidoglycan layer within the cell wall can be very diagnostic to its characterization. As shown below in Figure 1, the peptidoglycan layer exists as an interwoven network of alternating *N*-acetylglucosamine and *N*-acetylmuramic acid residues cross-linked by pentapeptide side chains to provide rigid support for the cell and adequate protection from hostile environments (Ingraham *et al*. 1983, Silhavy *et al*. 2010). Although variable between species, the pentapeptide side chain in Gram-positive bacteria typically exists as L-Ala—D-Glu—L-Lys—D-

Ala—D-Ala; differing from Gram-negative bacteria, where diaminopimelic acid generally replaces the third amino acid residue (Sarkar *et al* 2017). Such a network differs between the two categories, where the peptidoglycan layer may be as thin as 2 nm in Gram-negative species and as thick as 15-80 nm in Gram-positive species (Figure 2) (Ingraham *et al*. 1983).

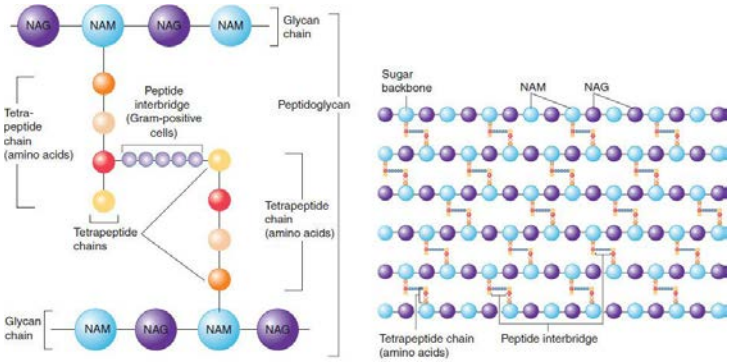

Figure 1. Basic structure of the peptidoglycan layer in bacterial cell walls (Ingraham *et al*. 1983).

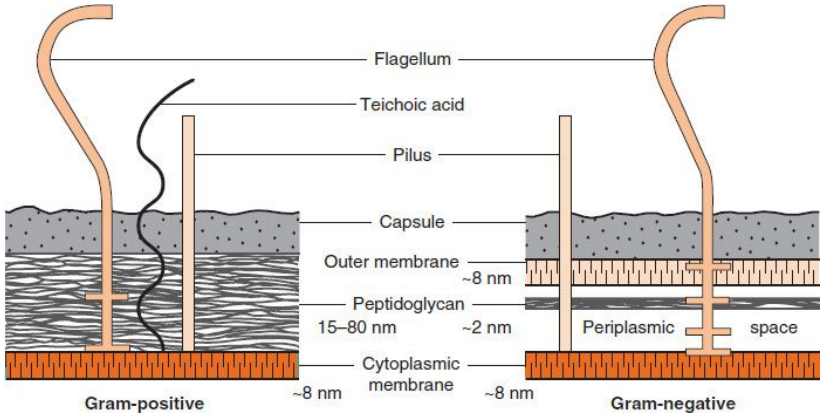

Figure 2. Cell walls of Gram-positive (left) and Gram-negative (right) bacteria (Ingraham *et al.* 1983).

Although a significant difference between the two species, it remained difficult to characterize the bacteria through only observation. Danish physician, Christian Gram, developed a simple four-step staining procedure on the basis of the peptidoglycan layer to easily visualize and distinguish a Gram-positive species from Gram-negative. Upon fixing a cell culture to a glass microscopy slide, crystal violet can be applied to

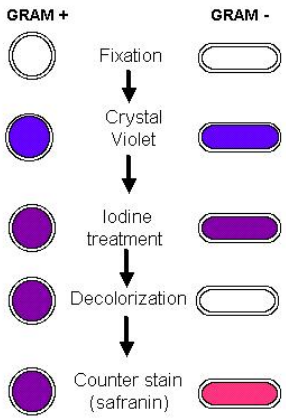

Figure 3. Gram-stain procedure.

saturate and stain each cell. The slide can then be flooded with iodine to act as a mordant in forming a crystal violet-iodine complex to intensify and increase the fastness of the stain. Washing the slide with an organic solvent, often acetone or ethanol, effectively extracts all of the crystal violet-iodine complex from thin-walled Gram-negative species and significantly less from the thick peptidoglycan layer of Gram-positive species. In such a way, Gram-negative species appear colourless and can then be stained pink with safranin or basic fuchsia, while Gram-positive species retain the original crystal violet-iodine complex and appear purple.

The presence of peptidoglycan in bacterial cells and its absence in mammalian cells makes it an ideal target for antibiotic treatment. The thick peptidoglycan layer in Gram-positive species can be effectively destroyed by treating with antibiotics which inhibit cell wall biosynthesis, commonly β-lactams or glycopeptides (Sarkar *et al.* 2017). Since peptidoglycan exists less prominently in Gram-negative cell walls, these species are often more difficult to treat. The specificity of an antibiotic to target primarily Gram-negative bacteria, rather than a breadth of species, has been highly sought after.

Secondary Metabolite Production

Although not universally produced by microbes (Malik 1980), secondary metabolites can serve their host as a means of protection against threatening organisms, as metal transporters, in symbiosis, as sexual hormones, and in differentiation mechanisms (Demain *et al*. 2000). Within their host system, the functions of secondary metabolites—namely pigments, alkaloids, toxins, antibiotics, gibberellins, carotenoids, etc.—are nil and are only truly beneficial once excreted (Malik 1980). The interest of this study lies in the *Streptomyces* specific production of bioactive secondary metabolites, many of which have functioned as antifungals, antivirals, antitumorals,

anti-hypersensitives, immunosuppressants, or antibiotics (Procopio *et al*. 2012). The broad application of these bioactive molecules stems from the array of metabolic pathways within a species, collectively referred to as its secondary metabolome (Avignone-Rossa *et al.* 2013).

The production of *Streptomyces* secondary metabolites occurs during the onset of developmental changes occurring in the species; these changes most prominently occur during the formation of aerial hyphae in solid cultures or in a liquid cultures stationary phase (Avignone-Rossa *et al*. 2013). Although not fully understood, nutrient exhaustion and the resulting growth rate stunt are thought to contribute in activating the secondary metabolism of *Streptomyces* (Avignone-Rossa *et al*. 2013).

The Iron Curtain Cave

The Iron Curtain Cave located near Chilliwack, British Columbia was discovered by caver Rob Wall in 1993 and was named accordingly for its iron-rich, decorative environment. The microbe involved in this study, *Streptomyces* sp. ICC1, was originally isolated 22.47 meters from the entrance of the cave, depicted as Point 1 in Figure 4, by Gosse *et al.* (2018). Previously established literature had noted that extreme cave environments, such as the Iron Curtain Cave, were found to commonly house microbial communities that actively produced secondary metabolites—many of which exhibited antimicrobial properties (Gosse *et al*. 2018). Cave-dwelling bacterial species, such as the *Streptomyces* sp. ICC1 strain of interest, are known to thrive in such desolate environments as a result of their unique physiology and specialized metabolic pathways (Cheeptham *et al*. 2013). In hopes to uncover a novel opportunity for the demand in pharmaceutical applications, this study has focused on the optimization and characterization of the

antimicrobial secondary metabolite(s) that are actively secreted from the *Streptomyces* sp. ICC1 strain.

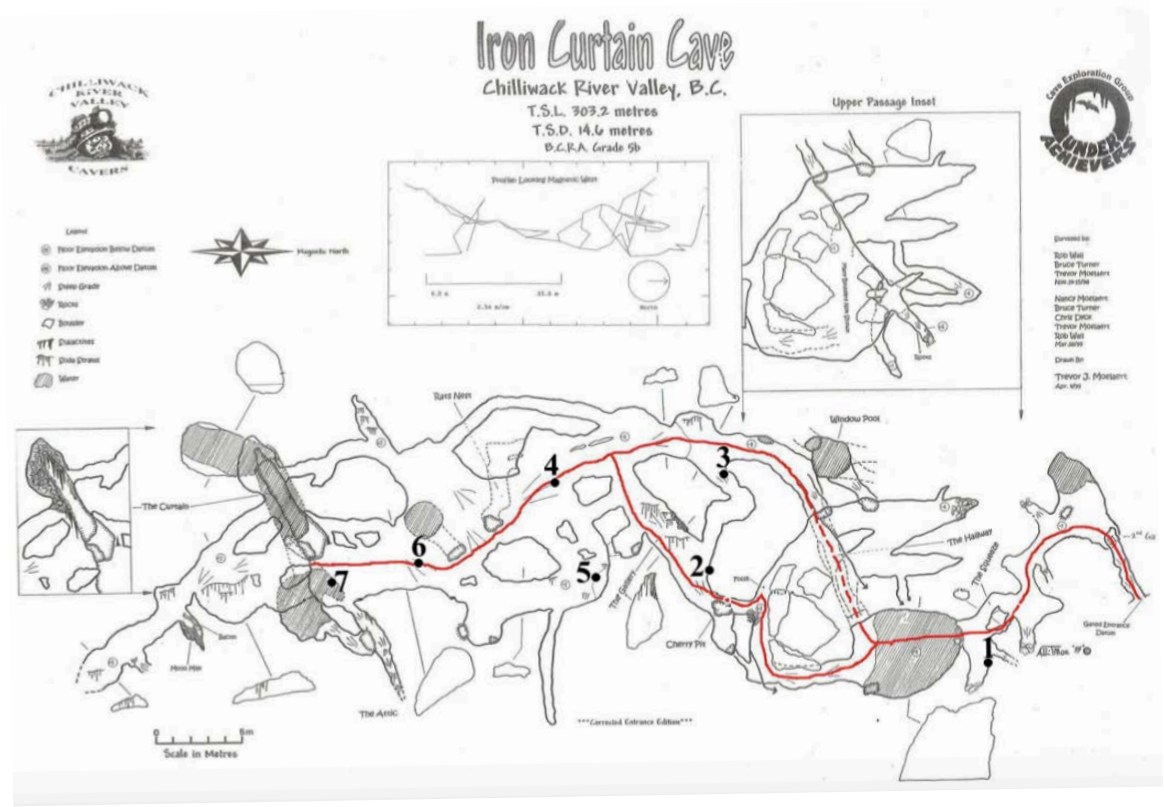

Figure 4. Map of the Iron Curtain Cave in Chilliwack, B.C. where the strain of interest, *Streptomyces* sp. ICC1 was collected at location Point 1. (Ghosh *et al*. 2017).

Found to be a highly filamentous Gram-positive bacilli, the morphological characteristics of *Streptomyces* sp. ICC1 mirror the general trends observed across the genus. The scanning electron micrograph generated by Ghosh *et al*. (2017), shown below in Figure 5, clearly depicts the dense rod-shaped filaments of the culture which contribute to its filamentous colonial appearance. The *Streptomyces* sp. ICC1 strain was found to align to 54% of the well-studied *Streptomyces lavendulae* strain CCM 3239 through 16S rRNA sequencing techniques (Gosse *et al*. 2018). More specifically, Illumina MiSeq analysis and *de novo* genome assembly found the *Streptomyces* sp. ICC1 genome to consist of 9,034,309 base pairs of which 72% were guanine and

cytosine nucleotide base pairs (Gosse *et al*. 2018). Phylogenetically, the *Streptomyces* genus are known to possess a genome rich with guanine and cytosine bases in comparison to other bacterial species (Procopio *et al*. 2012). In the pharmaceutical industry, over 80% of the bacterial sourced antimicrobial products are derived from members of the *Streptomyces* genus (Procopio *et al*. 2012), with the ICC1 strain being no exception.

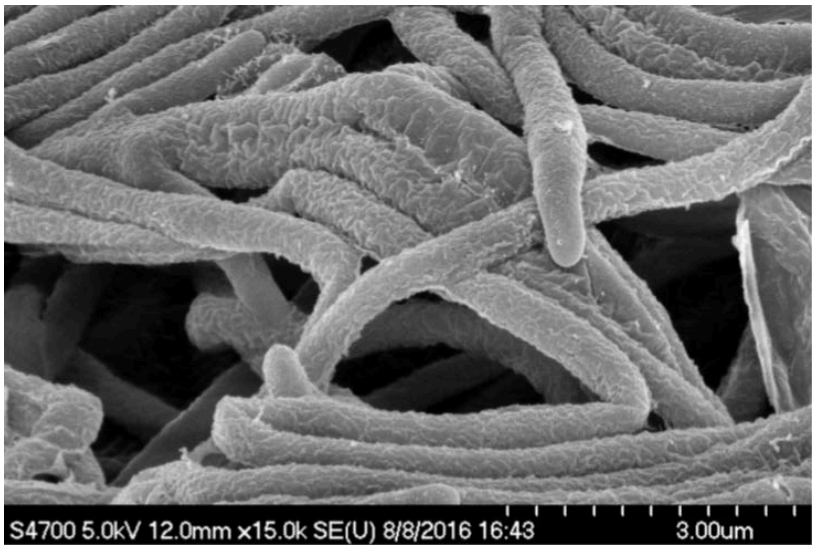

Figure 5. Scanning electron micrograph of *Streptomyces* sp. ICC1 retrieved from the Iron Curtain Cave (Ghosh *et al*. 2017).

In this study, aseptic bioassay techniques and instrumental analyses were employed to observe antimicrobial performance against both Gram-positive and Gram-negative target organisms, specifically laboratory and multi-drug resistant strains of *Escherichia coli* and *Staphylococcus aureus*. The bioactive secondary metabolite(s) produced by the cave-dwelling *Streptomyces* sp. ICC1 strain were separated out from culture via multiple liquid-phase organic solvent and water extractions. Prominent bioactivity was consistently observed when such extractions were performed with diethyl ether. The bioactive compound(s) were further separated via analytical and preparative reversed-phase high performance liquid chromatography (HPLC) techniques, followed by structural elucidation via one-dimensional proton nuclear magnetic

resonance (NMR) spectroscopy. The preliminary findings of this study indicate that the antimicrobial secondary metabolite(s) are relatively hydrophobic/non-polar and potentially peptidic. Future work to further the understanding of the bioactive compound(s) involve additional instrumentation techniques, such as carbon-13 NMR spectroscopy and mass spectrometry, as well as unraveling their mechanism of action against tested pathogenic target organisms.

MATERIALS AND METHODS

Recovery from Dormant Colony

The *Streptomyces* sp. ICC1 strain was streaked for isolated colonies on nutrient agar from a single dormant colony. Agar plates were streaked in triplicate and incubated overnight at 15°C—later found to be an optimal temperature condition for growth and secondary metabolite production for *Streptomyces* sp. ICC1. Each plate was parafilmed and stored at 4°C to inhibit continual growth. Colonies were taken from these stock plates in all further culturing conditions.

Optimization of Growth Conditions

To determine the optimal growth conditions for *Streptomyces* sp. ICC1, three different mediums were tested at three temperatures. Performed in triplicate, the cultures were grown up in 15 mL aliquots of either nutrient broth, Reasoner's 2A broth, or Hickey Tresnar broth and incubated at either 8°C, 15°C, or 37°C at 150 rpm. OD_{600} measurements were collected in 12 hour increments for 8 days.

Optimization of Bioassay Zones of Inhibition

Based on the understanding that the *Streptomyces* sp. ICC1 strain grows most rapidly in nutrient broth conditions, all bioassays were performed first using molten nutrient agar. Fresh broth and agar media were inoculated or streaked from a single colony, where bioactivity was tested for every third day using both plug-assays and Kirby-Bauer disk diffusion assays. Plug-assays and Kirby-Bauer assays were performed from the previously tested conditions: agar and broth cultures of nutrient media, Reasoner's 2A, and Hickey Tresnar grown at 15°C.

Kirby-Bauer disk diffusion assays required soaking 6mm sterilized paper disks with the either filtered or unfiltered supernatant of nutrient broth, Reasoner's 2A broth, and Hickey Tresnar broth samples. Prior to saturation of the disks, the samples were centrifuged for 20 min at 10,000 rpm and the supernatant samples were then divided into corresponding filtered and unfiltered samples. Chosen samples were filtered via sterile hydrophilic low-protein-binding polyethersulfone membrane filters of pore size 0.22 μm.

Bioassay Screening for Antimicrobial Activity

A target organism of choice was cultured overnight at 37°C to 0.600-0.900 OD_{600} to ensure active logarithmic division. The bacterial targets employed in the bioassay screening protocols were namely laboratory *Escherichia coli* #59, multi-drug resistant *Escherichia coli* #15-124, laboratory *Staphylococcus aureus*, and methicillin-resistant *Staphylococcus aureus* ATCC-43300.

An aliquot of *Streptomyces* sp. ICC1 broth culture incubated at 15°C for 5-40 days in nutrient broth at 150 rpm was retrieved and centrifuged at 10,000 rpm for 20 min. The supernatant was collected and filtered through sterile hydrophilic low-protein-binding polyethersulfone membrane syringe filters with 0.22 μm pore size. Various liquid extractions were performed on aliquots of the filtrate in 1:1 parts broth to diethyl ether, ethyl acetate, straight-chain hexanes, or 1-octanol. Autoclaved 6 mm paper disks were saturated with either aqueous filtrate or organic solvent post-extraction and dried completely prior to bioassay addition.

Bioassay screening was performed in sterile 15 mm x 150 mm polystyrene Petri dishes after exposure to ultraviolet radiation. Eighty mL of autoclaved molten nutrient agar was inoculated with 1% volume to volume of the exponentially dividing target organism, OD_{600} between 0.600-0.900. The Kirby-Bauer disk diffusion method was employed in all bioassay

screening. All bioassay screening was performed within a biosafety cabinet to mitigate contamination and undesired bacterial exposure. The bioassay plates were incubated for 24 h at 37°C for optimal growth of the target bacterial lawn. The presence or absence of zones of inhibition were recorded for each experimental condition.

Active Compound(s) Separation and Preliminary Structural Analysis

The organic layer of the diethyl ether and broth liquid extraction was known to possess antimicrobial activity against the previously mentioned target organisms. Liquid extractions with diethyl ether were performed on aliquots of the *Streptomyces* sp. ICC1 broth culture collected every 3 days between 5 and 40 days of incubation at 15°C at 150 rpm. The organic layers from each extraction were combined and evaporated. For injection into the Agilent 1220 Infinity II high performance liquid chromatography (HPLC) system, the active compound(s) were resuspended from the dry flasks in 10 mL of HPLC-grade methanol.

The bioactive compound(s) were separated according to the analytical reversed-phase HPLC conditions summarized in Table 1. Following method development and analytical HPLC analysis, individual components were then collected via the preparative HPLC conditions further listed in Table 1. The resulting four separated components were divided among Eppendorf tubes and the eluent evaporated on a Vacufuge® 5301 Centrifugal Vacuum Concentrator at 45°C. One sample from each separation was resuspended in deionized 18MΩ water and analyzed for antimicrobial activity via additional Kirby Bauer disk diffusion assays. Remaining samples were resuspended in either chloroform or 90:10 sodium phosphate buffer and deuterium oxide for structural elucidation with one-dimensional proton nuclear magnetic resonance (NMR) spectroscopy via a 500 MHz Bruker Avance AMIII 500 Spectrometer.

Table 1. Analytical and preparative HPLC parameters for compound separation.

	Analytical HPLC Parameters	Preparative HPLC Parameters
Instrument	Agilent 1220 Infinity HPLC	Waters HPLC 486
Column	Kinetex® 2.6 μm EVO C18 100Å	Phenomenex® Jupiter 10u C18 300Å
Dimensions	100 x 3.0 mm	250 x 21.20 mm
Detector	195, 272 nm	272 nm
Flow Rate	0.4 mL/min	5 mL/min
Injection Volume	5.0 μL	1.0 mL
Eluent	A: 5 mM NH_4OAc in 18 MΩ H_2O B: Acetonitrile	
Program Gradient	1-21 min 90% A 10% B 21-31min 100% B 31-40min 90% A 10% B	

Table 2. NMR parameters for structural elucidation.

Instrument	Bruker Avance AMIII 500 Spectrometer
Operating Frequency	500 MHz
Solvent	$CDCl_3$
Number of Scans	128

RESULTS

Streptomyces sp. ICC1 Growth Optimization

Streptomyces sp. ICC1 was subjected to three different media conditions and three temperatures to optimize the bacterial growth and secondary metabolite production of the cave strain. The OD_{600} measurements, estimating bacterial concentration, were found to be highest in nutrient broth conditions when incubated at 15°C, 150 rpm. While the nutrient broth cultures were found to have the greatest concentration at each temperature condition, the growth rate was significantly repressed at 8°C and more so at 37°C. Bacterial growth was minimal in Reasoner's 2A broth; likewise, Hickey Tresnar broth conditions showed no growth at each temperature after 8 days post-inoculation.

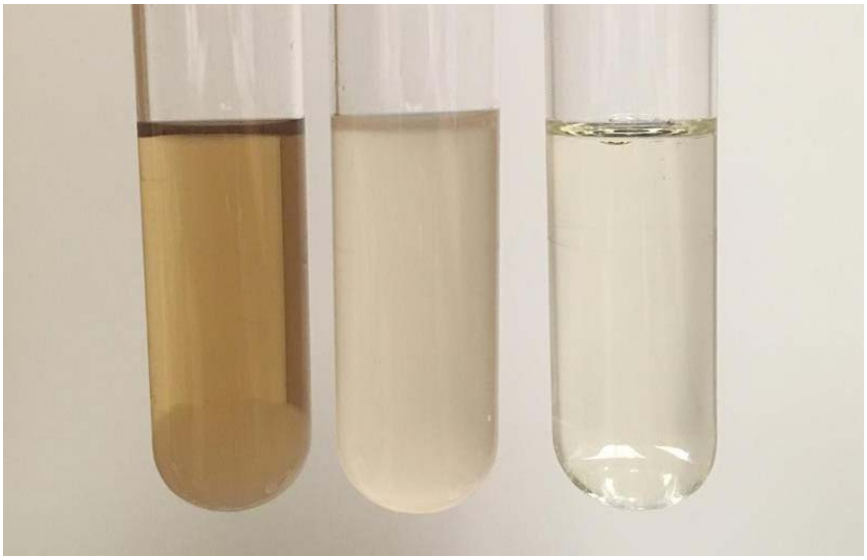

Figure 6. Brown pigment change and considerable *Streptomyces* sp. ICC1 growth following 8 days post-inoculation at 15°C, 150 rpm in nutrient broth (left). Bacterial growth considerably less in Reasoner's 2A broth (middle), and minimal in Hickey Tresnar (right).

Additionally, a brown pigment change in media was consistently observed after 5 days of incubation at 15°C and 150 rpm in nutrient broth. The evident pigment change from clear to distinct brown has been thought to correlate to secondary metabolite production by the cave strain,

since bioactivity has been observed only thereafter. The shift in media colour was observed earliest in nutrient broth after 5 days, later in Reasoner's 2A broth after 12 days, and even later so in Hickey Tresnar broth after 28 days post-inoculation.

Following incubation of the *Streptomyces* sp. ICC1 culture in nutrient broth at 15°C, a conventional Gram-stain confirmed the cave-dwelling bacterium to possess filamentous Gram-positive bacilli properties, shown below in Figure 2. These observations were in agreeance with the findings of Ghosh *et al*. (2017) in their scanning electron microscopy analysis of a *Streptomyces* sp. ICC1 sample.

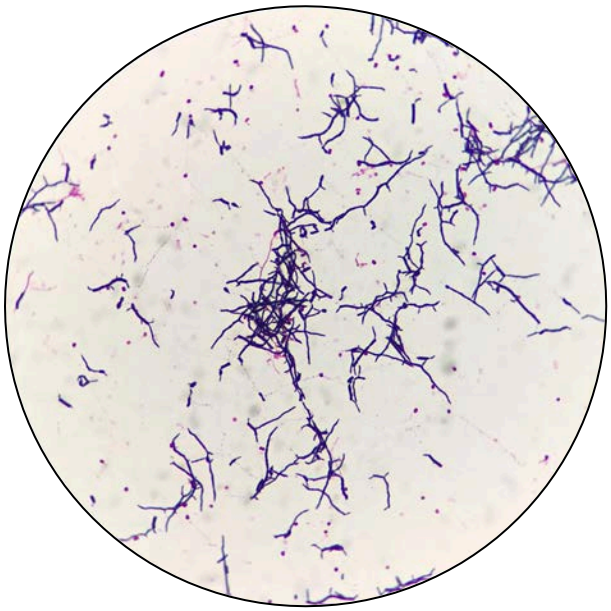

Figure 7. *Streptomyces* sp. ICC1 with filamentous Gram-positive bacilli properties at 1000X magnification.

Optimization of Bioassay Zones of Inhibition

Plug-assays and Kirby-Bauer disk diffusion assays were performed on molten nutrient agar. Bioactivity was not observed until 6 days post-inoculation, suggesting secondary metabolite production must occur between days 3-6. Through identically repeated analysis, it was later determined that antimicrobial activity via secondary metabolites begins 5 days post-inoculation.

The *Streptomyces* sp. ICC1 colonies grown on nutrient agar produced a larger zone of inhibition on all target organism bacterial lawns. In contrast, the zones of inhibition observed on Hickey Tresnar agar and Reasoner's 2A agar from the colonies were relatively similar, however both were consistently smaller than the zones established from nutrient agar. The diameter of the zone of inhibition steadily increased until approximately 72 hours post-incubation, at which point the change in diameter was less significant and eventually showed no change after 150 hours. Of note, these times may have varied among the bacterial lawns. All plug-assays produced the characteristic brown pigment from the *Streptomyces* culture after 72 hours when incubated at 15°C. An identical procedure was carried out to incubate the bioassay plates at 37°C, however no zones of inhibition were observed as well as no brown pigmentation. After producing these results in triplicate, the study eliminated the 37°C incubation condition.

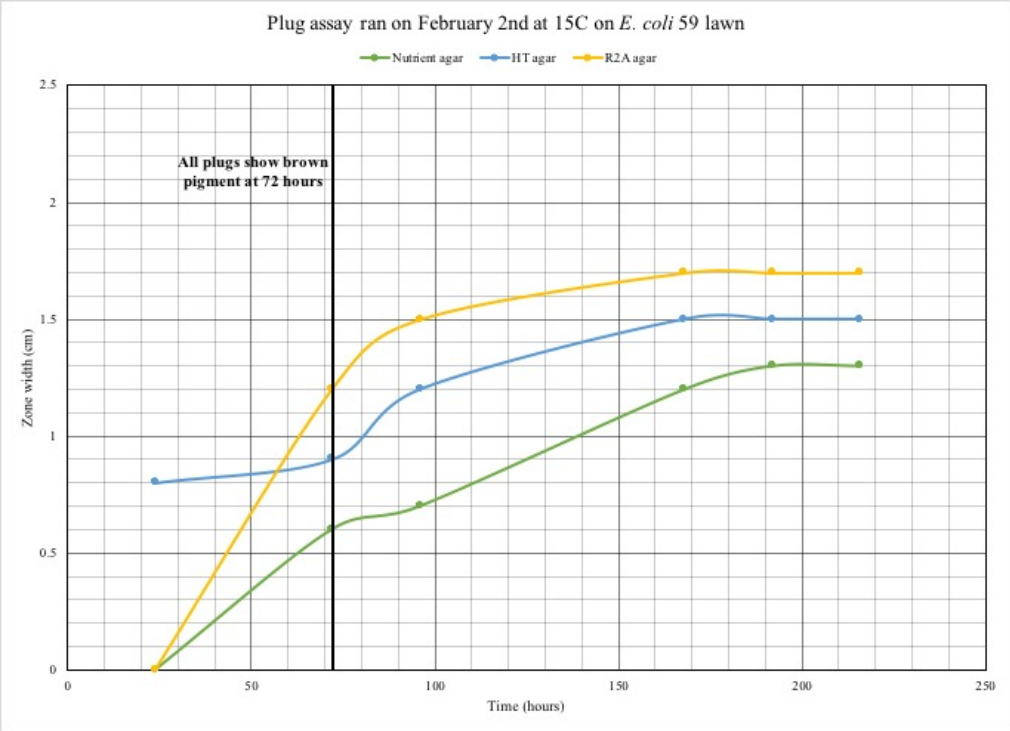

Figure 8. Diameter of zone of inhibition on an *Escherichia coli* #59 bacterial lawn at 15°C by nutrient agar plug-assay.

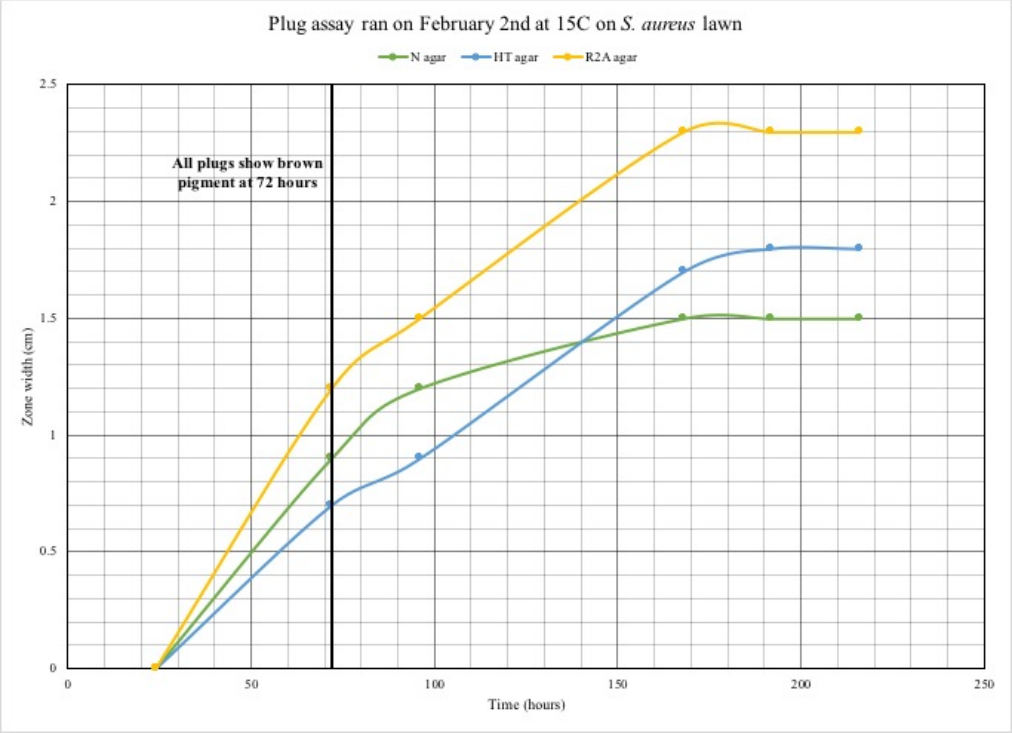

Figure 9. Diameter of zone of inhibition on a *Staphylococcus aureus* bacterial lawn at 15°C by nutrient agar plug-assay.

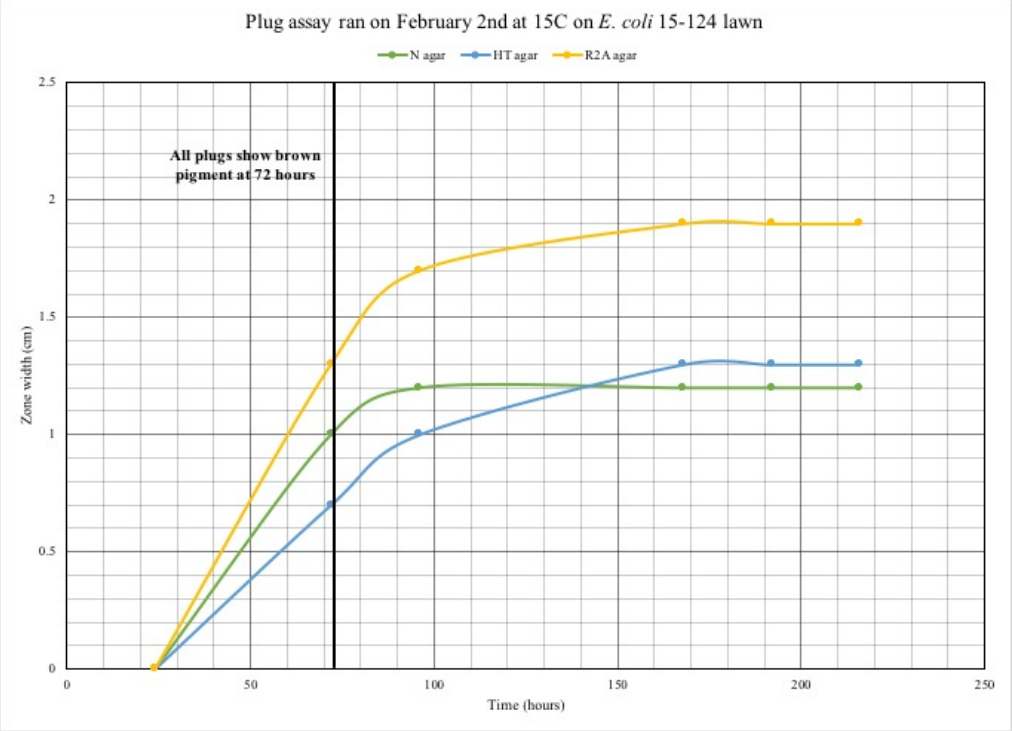

Figure 10. Diameter of zone of inhibition on a multi-drug resistant *Escherichia coli* #15-124 bacterial lawn at 15°C by nutrient agar plug-assay.

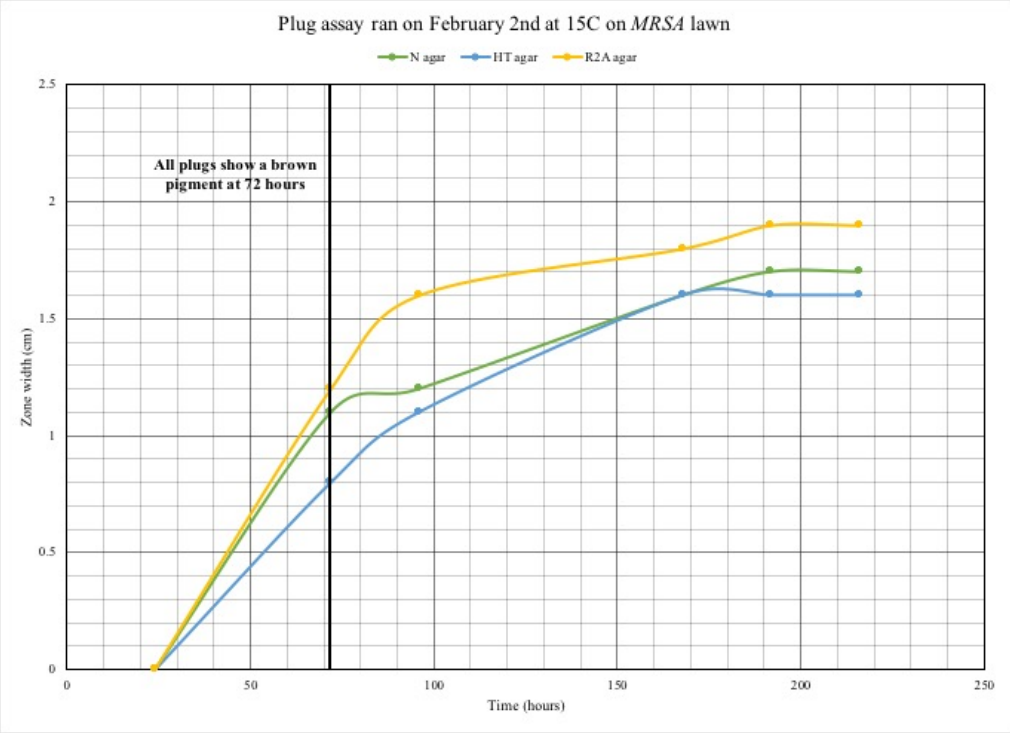

Figure 11. Diameter of zone of inhibition on a methicillin-resistant *Staphylococcus aureus* bacterial lawn at 15°C by nutrient agar plug-assay.

The Kirby-Bauer disk diffusion assay results were less consistent across the four target organism bacterial lawns. On all except the laboratory strain of *Escherichia coli* #59 bacterial lawns, bioactivity was observed via a zone of inhibition from both filtered and unfiltered nutrient broth supernatant samples. No bioactivity was observed when testing the supernatant samples from the Hickey Tresnar grown culture. However, the Reasoner's 2A unfiltered supernatant showed zones of inhibition on both laboratory and methicillin-resistant strains of *Staphylococcus aureus*. The filtered Reasoner's 2A supernatant showed no bioactivity, similar to the Hickey Tresnar.

Figure 12. Diameter of zone of inhibition on an *Escherichia coli* #59 bacterial lawn at 15°C by Kirby Bauer disk diffusion assay.

Figure 13. Diameter of zone of inhibition on a *Staphylococcus aureus* bacterial lawn at 15°C by Kirby Bauer disk diffusion assay.

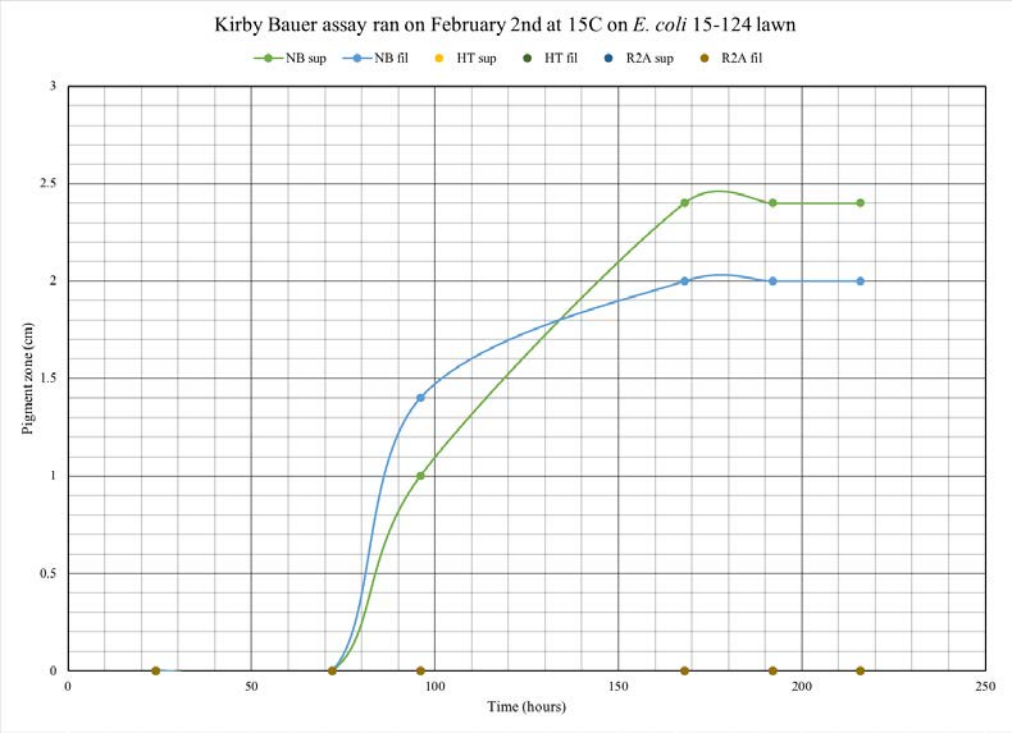

Figure 14. Diameter of zone of inhibition on a multi-drug resistant *Escherichia coli* #15-124 bacterial lawn at 15°C by Kirby Bauer disk diffusion assay.

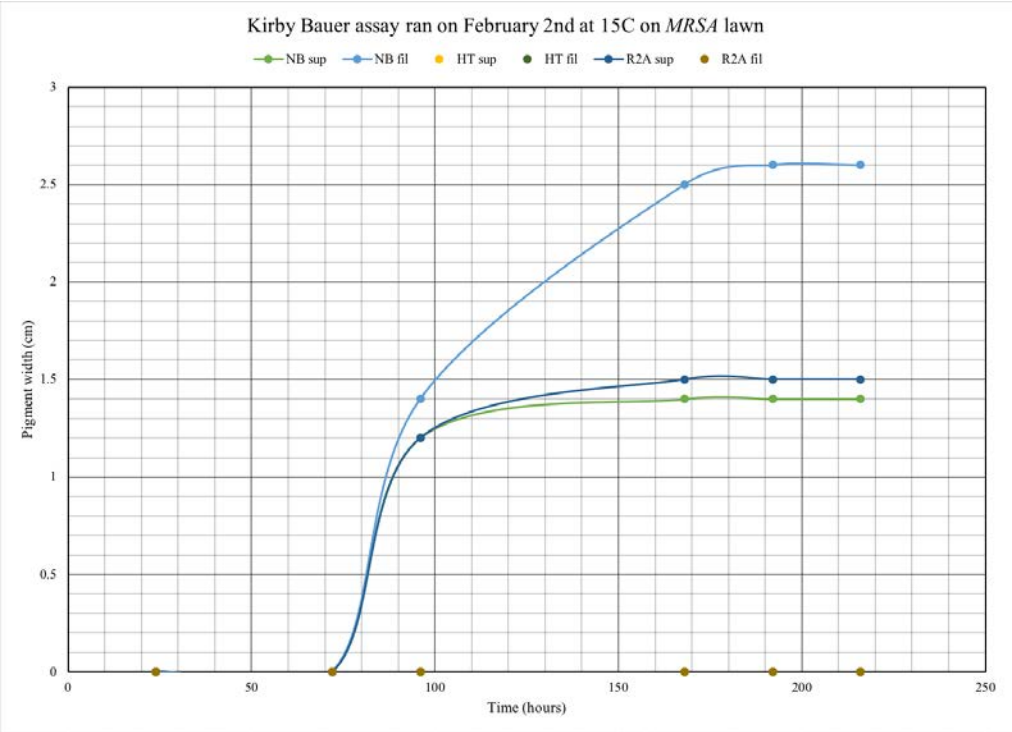

Figure 15. Diameter of zone of inhibition on a methicillin-resistant *Staphylococcus aureus* bacterial lawn at 15°C by Kirby Bauer disk diffusion assay.

Antimicrobial Activity Following Organic Solvent Extractions

Following observed antimicrobial activity after 5-40 days post-inoculation in nutrient broth, liquid organic solvent extractions were performed to elucidate the relative polarity of the bioactive antimicrobial secondary metabolite(s). Extractions were performed with four organic solvents, namely diethyl ether, ethyl acetate, hexane, and 1-octanol, and bioactivity was assessed post-extraction to determine the partition behaviour of the bioactive compound(s). The results from the performed extractions in the various solvents are summarized below in Table 2. As listed, the extractions were unsuccessful when using reagent-grade ethyl acetate, as no activity was present in either the organic nor the aqueous layer post-extraction. The hexane-water extractions were also deemed unsuccessful, as bioactivity against the target organisms was inconsistently observed. However, bioactivity was observed consistently in the organic layer of the diethyl ether-water extractions, Figure 3, and in the aqueous layer of the octanol-water extractions.

Table 3. Bioactivity post-extraction using four different organic solvents.

Solvent	Organic Layer Activity Observed	Aqueous Layer Activity Observed
Diethyl Ether	Yes +++	No
Ethyl Acetate	No	No
Hexane	No	Yes +
1-Octanol	No	Yes ++

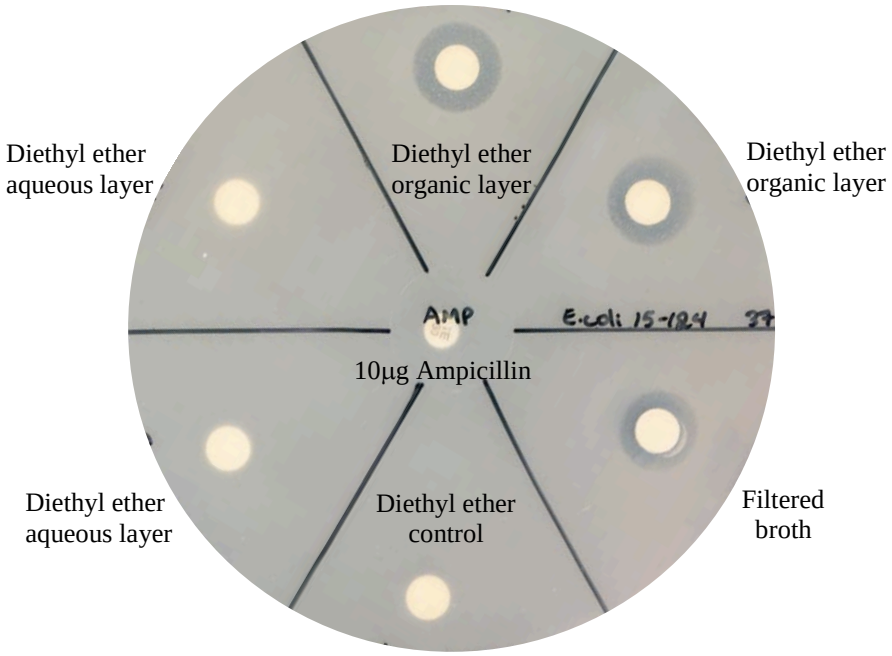

Figure 16. Kirby-Bauer disk diffusion assay against multi-drug resistant *Escherichia coli* #15-124 showing bioactivity post-extraction with diethyl ether.

Compound Separation via Reversed-Phase HPLC

Method development of the reversed-phase HPLC protocol was performed to achieve adequate separation among the various components. The resulting chromatograms are depicted below in Figures 4A and 4B. By measuring absorbance at 195 nm and 272 nm via a photodiode array detector, it was determined that the program gradient summarized above in Table 1 allowed for the highest resolution among the eluting peaks. Although lower in relative absorbance intensity, 272 nm delivered a “cleaner” chromatogram and was chosen as the wavelength for later preparative HPLC analysis. It was critical to achieve relatively high resolution prior to sample collection to increase the samples purity. While baseline resolution was difficult to achieve for each individual component, Figure 4B demonstrated adequate separation for performing collections.

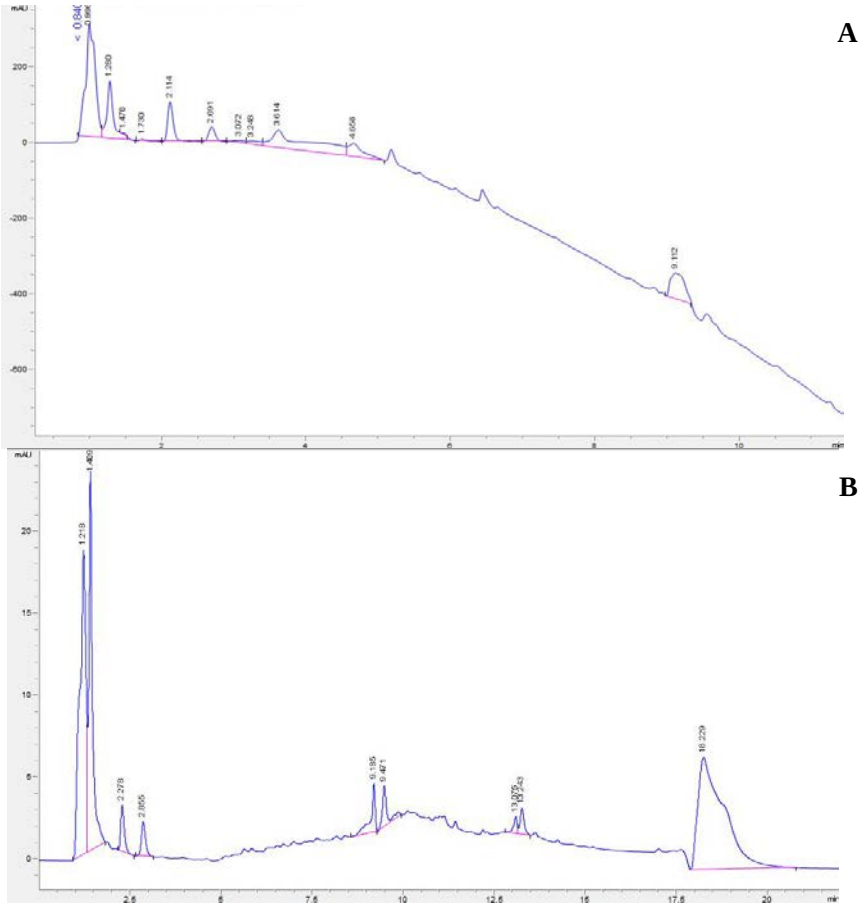

Figure 17. Analytical reversed-phase HPLC chromatograms of bioactive secondary metabolite(s) in methanol at 195 nm (A) and 272 nm (B) detection.

As an additional method of determining maximum absorbance for the biological sample, a three-dimensional chromatogram of the bioactive secondary metabolite(s) in methanol was created from the absorbance readings of 190 nm to 400 nm by the photodiode array detector. It was noteworthy that although 195 nm delivered the maximum absorbance for the initial components—clearly depicted below in Figure 5, the resolution between peaks was not as high as that of the peaks that absorbed at 272 nm. Furthermore, the peak appearing between 8 min and 9 min was not absorbed at 195 nm but was observed at 272 nm.

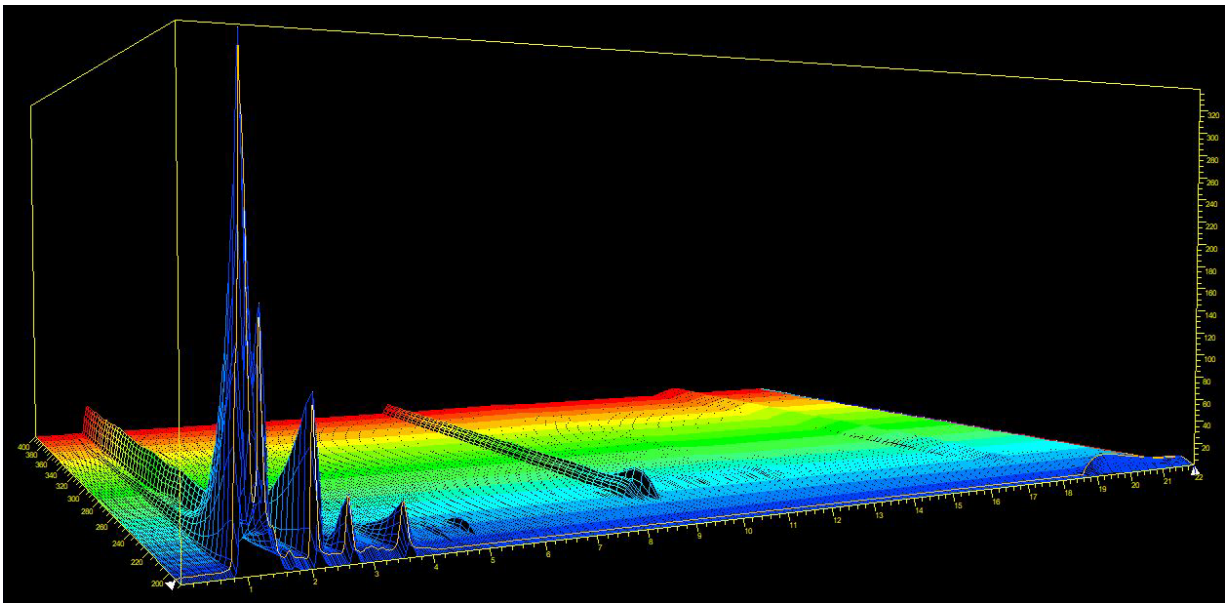

Figure 18. 3-D chromatogram of bioactive secondary metabolite(s) showing absorbance from 190-400 nm via photodiode array detection.

The preparative reversed-phase HPLC chromatogram, shown below in Figure 6, appeared relatively different from that of the analytical chromatogram as a result of the different column compositions. Due to the non-polar stationary phase of the Phenomenex® Jupiter 10u C18 column, polar substituents are the first to elute due to their high affinity for the polar mobile phase. It may be inferred then that Peaks 1 and 2 depicted in Figure 6 are relatively polar components due to their short retention time. Furthermore, the broadness and multiple peaks that appear are indicative of several underlying components residing within each peak.

Due to the high volume capacity of the preparative Phenomenex® Jupiter 10u C18 column, it can be reasoned that the Peak 3 collection likely was eluted in 90% 5 mM ammonium acetate buffer and 10% acetonitrile. Similarly, the Peak 4 collection was likely eluted in 100% acetonitrile. The non-polar nature of acetonitrile can be thought to "clean" off the column by interacting with the non-polar substituents that have a high affinity for the columns stationary phase. As a result, Peak 4 can be reasoned to be quite impure due to the several components contributing to the broad

peak. In future, the colossal peak could be separated into its individual components by lengthening the program gradient and allowing elution in a high concentration of aqueous buffer, such as the previously used 90:10 ratio.

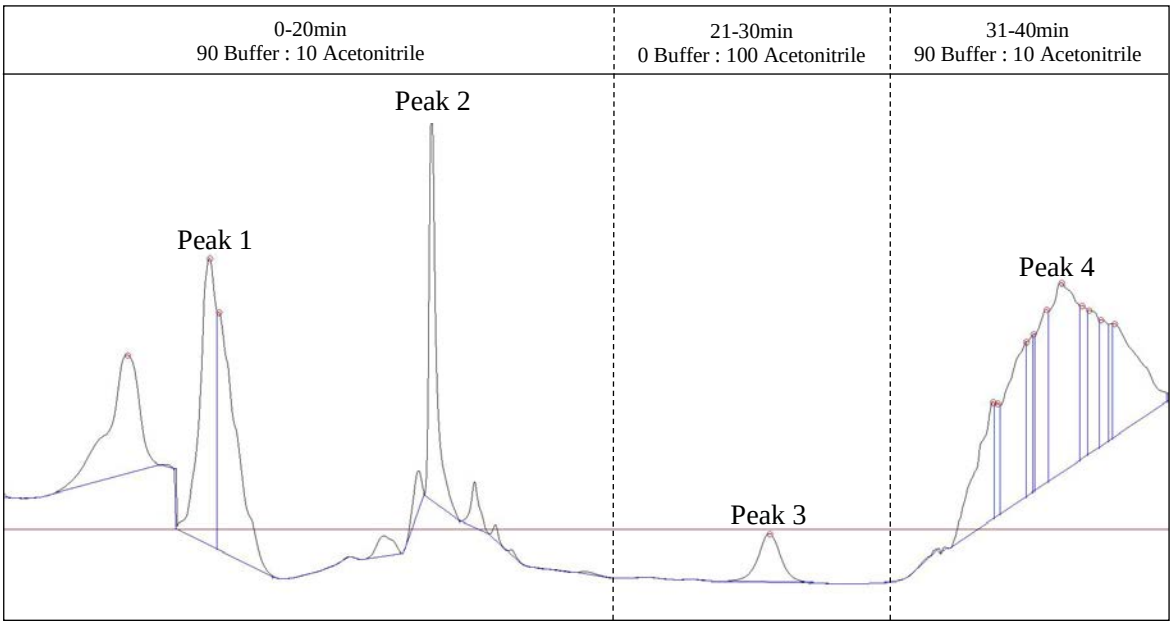

Figure 19. Preparative reversed-phase HPLC chromatogram of bioactive secondary metabolite(s) in methanol with program gradient.

The bioactivity of each of the four peak sample collections was tested via Kirby-Bauer disk diffusion assays following the evaporation of all HPLC eluent. As shown below in Figure 7, the bioactive secondary metabolite(s) were evidently separated into Peak 2 and Peak 4 during the preparative reversed-phase HPLC analysis. The clear zones of inhibition against the multi-drug resistant strain *Escherichia coli* #15-124 are indicative of antimicrobial agents having been absorbed into the applied paper disk. These peak samples were further analyzed for structural elucidation via IR and one-dimensional proton NMR analysis.

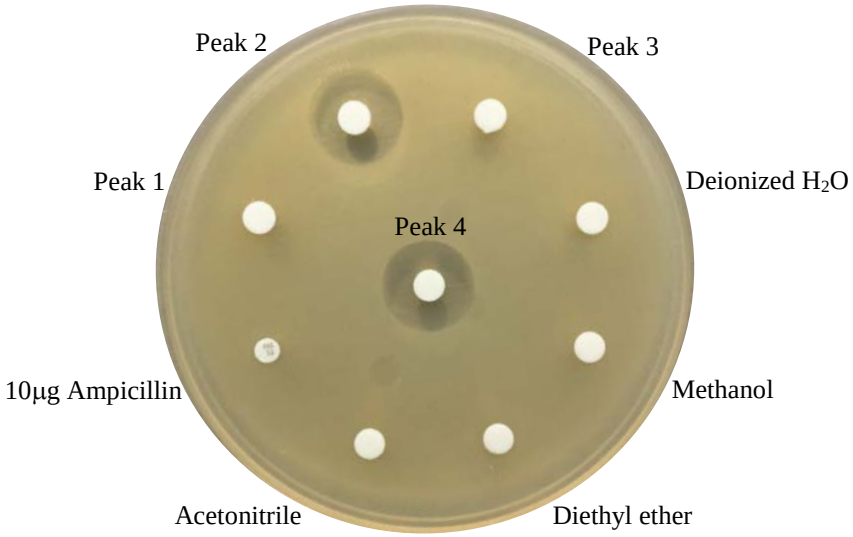

Figure 20. Kirby-Bauer disk diffusion assay against multi-drug resistant *Escherichia coli* #15-124 showing antimicrobial activity from Peak 2 and 4 of preparative HPLC collections.

Structural Elucidation of Bioactive HPLC Collections by IR and 1-D ^{1}H-NMR

The vacufuged samples from the Peak 2 and 4 collections were resuspended in 9-parts sodium phosphate buffer and 1-part deuterium oxide and were observed to be very soluble. Noteworthy, the vacufuged samples exhibited a similar brown pigmentation when dry to that of the original pigmentation observed during secondary metabolite production (after 5 days). Of interest, 1-D ^{1}H NMR analysis of these samples did not provide any structural information as no peaks were present aside from the suppressed water signal, likely due to minimal sample.

Other vacufuged samples from Peaks 2 and 4 were dissolved in deuterated chloroform ($CDCl_3$) and analyzed. The spectrum obtained from analyzing Peak 2 in $CDCl_3$ at 128 scans by the 500 MHz Bruker NMR spectrometer can be seen below in Figure 8A. Sections of the spectrum have been further zoomed in on to aid in visualization of individual peak splitting patterns, Figures 8B-8D. As seen in Figure 8B, a clean doublet appears around 2.25 ppm; two clean singlets at 2.05 and 2.1 ppm; the water peak at approximately 1.56 ppm; and two crude multiplets at 0.8 ppm and

1.25 ppm. The latter two signals are likely a result of CH_2 and CH_3 protons, due to their upfield and highly shielded placement on the spectrum. A clean triplet can be observed in Figure 8C at approximately 5.6 ppm, suggestive of possible alkene protons. Additionally, the complicated splitting observed in the peaks appearing from 3.8-4.4 ppm may be a result of protons being nearby deshielding/electron-withdrawing groups, such as alkenes or electronegative oxygen or nitrogen atoms. Figure 8D shows the large deuterated chloroform solvent peak at 7.26 ppm. The doublet at approximately 7.15 ppm and the two singlets at approximately 7.05 ppm and 7.45 ppm, as well as the peaks superimposed beneath the solvent peak, likely correspond to aromatic protons due to their downfield/deshielded placement on the spectrum. Furthermore, additional scans should be taken, or the sample concentrated, to determine if there are true singlets arising at approximately 8.75 and 9.10 ppm. These signals could be indicative of deshielded amide protons, hinting that the bioactive secondary metabolite(s) may possess an indole ring.

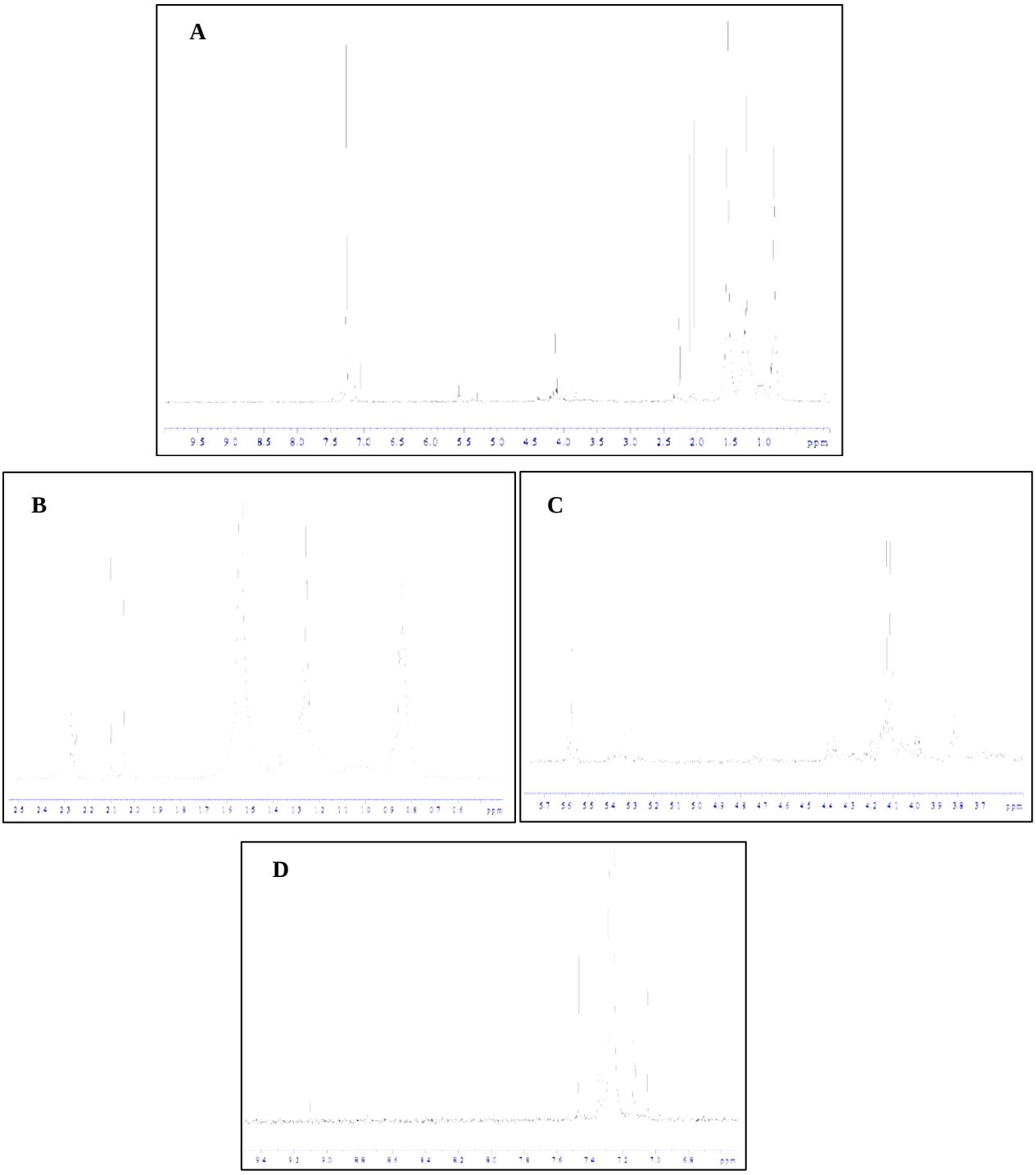

Figure 21. 1-D ^{1}H NMR spectra of Peak 2 dissolved in deuterated chloroform, NS=128.

DISCUSSION

Through extensive Kirby-Bauer disk diffusion antimicrobial assays, the bioactive secondary metabolite(s) produced by *Streptomyces* sp. ICC1 have been notably effective against both Gram-positive and Gram-negative target organisms—primarily laboratory and multi-drug resistant strains of *Escherichia coli* and *Staphylococcus aureus*. The bioactive compound(s) should be applied against other infectious bacterial organisms to observe their effectiveness and limitations.

Following liquid organic solvent extractions with the aqueous broth culture, bioactivity was maintained in the organic, non-polar layer of the diethyl ether-water extractions and in the aqueous, polar layer of the 1-octanol-water extractions. Diethyl ether—essentially non-polar and insoluble in water—has a bent molecular structure that creates a small dipole moment and can therefore be used to isolate both polar and non-polar compounds in aqueous extractions. Since non-polar compounds tend to be more soluble in diethyl ether, it may be inferred from the organic extraction results that the secondary metabolites are also non-polar in nature. However, the bioactive compound(s) tendency to prefer the aqueous layer of the straight chain 1-octanol-water extractions actively suggests the secondary metabolites have polar characteristics, as they do not interact with the straight carbon chains of 1-octanol. Organic solvent extractions with ethyl acetate should be reinvestigated to understand the loss of activity post-extraction.

Upon confirmation that bioactivity was preserved through the liquid organic solvent extractions, analytical and preparative reversed-phase high performance liquid chromatography analysis revealed several polar and non-polar substituents within the diethyl ether extraction. Those peaks which eluted early, specifically Peaks 1 and 2, in the polar mobile phase were reasoned to possess more of a hydrophilic, polar nature. Whereas those peaks which eluted later due to a higher affinity for the non-polar stationary phase, Peaks 3 and 4, are thought to exhibit

more hydrophobic, non-polar characteristics. From additional Kirby-Bauer disk diffusion assays, it was determined that the antimicrobial secondary metabolite(s) from *Streptomyces* sp. ICC1 were separated into Peaks 2 and 4. It remains unclear whether these peaks possess entirely different bioactive molecules or if there was carry-over from the high-volume capacity of the preparative Phenomenex® Jupiter C18 column. A longer program gradient at a higher aqueous concentration should be manipulated in future work to improve the resolution of individual components.

A more concentrated sample from the Peak 2 and Peak 4 collections should be analyzed via one-dimensional proton nuclear magnetic resonance spectroscopy with a high number of scans to provide a more accurate representation of the molecular composition. Increasing the concentration of the analyzed sample may reveal additional peaks or intensify those present, such as the highly deshielded signals present in the amide region. Observation of amide protons, as well as the present aromatic and other sp^2/sp^3 hybridized alkyl protons could ultimately suggest a proteinaceous nature to the bioactive *Streptomyces* sp. ICC1 secondary metabolite(s). Additionally, samples may be dissolved in other deuterated solvents prior to NMR analysis. The compound(s) may be more soluble in dimethylsulfoxide, considered a universal solvent, than in the previously employed deuterated chloroform or sodium phosphate buffer/deuterium oxide combination.

CONCLUSIONS AND FUTURE WORK

The turn of the 20th century brought a demand for pharmaceutical development through antibiotic research and application. While microorganisms continue to evolve on a day to day basis, mankind risks the chance of falling behind their evolutionary progress in developing resistance. Hence, the research that encompasses how and which microbes naturally produce antimicrobial compounds should be considered imperative. The isolation of these bioactive

molecules has given rise to a significant portion of all the powerful and commercially available antibiotics used thus far against known infectious strains.

Further instrumental analysis should be executed on the purified samples, primarily ^{13}C NMR and mass spectrometry, to elucidate the bioactive molecular structure of the compound(s). Additionally, information regarding the minimum inhibitory concentration of the produced bioactive molecule(s) should be investigated against several target strains, both Gram-positive and Gram-negative. Together, these findings can be compared to other commercially available secondary metabolites produced by the *Streptomyces* genus to assess the possible novelty of the compound(s).

Although the most common antibiotics are those which target Gram-positive bacteria, the *Streptomyces* sp. ICC1 cave strain should be further studied for its effectiveness against other Gram-negative species than those mentioned. The resilient physiology and metabolic pathways that exist within cave-dwelling species, much like in *Streptomyces* sp. ICC1, offer an alternative to harmful chemical exposure and synthetic drug design. Continual research in the area of bioactive metabolite production by desolate environment microbial communities must be executed to uncover the possible cures that may reside within.

LITERATURE CITED

Avignone-Rossa C, Kierzek AM, Bushell ME. 2013. Secondary Metabolite Production in *Streptomyces*. Springer Encyclopedia of Systems Biology, DOI: 10.1007/978-1-4419-9863-7_1164.

Bhullar K, Waglechner N, Pawlowski A, Koteva K, Banks ED, Johnston MD, Barton HA, Wright GD. 2012. Antibiotic Resistance Is Prevalent in an Isolated Cave Microbiome. PLoS ONE 7(4): e34953.

Cheeptham N. 2013. "Advances and challenges in studying cave microbial diversity," in *Cave Microbiomes: A Novel Resource for Drug Discovery*, ed. N. Cheeptham. Spring Briefs in Microbiology, 1-34.

Demain AL, Fang A. 2000. The natural functions of secondary metabolites. Advances in Biochemical Engineering/Biotechnology 69: 1-39.

Ghosh S, Paine E, Wall R, Kam G, Lauriente T, Sa-ngarmangkang P, Horne D, Cheeptham N. 2017. In Situ Cultured Bacterial Diversity from Iron Curtain Cave, Chilliwack, British Columbia, Canada. Diversity 9(3): 1-15.

Gosse JT, Ghosh S, Sproule A, Overy DP, Cheeptham N, Boddy CN. 2018. Whole genome sequencing and metabolomic study of cave *Streptomyces* isolates ICC1 and ICC4. Frontiers of Microbiology, DOI: 10.3389/fmicb.2019.01020.

Ingraham JL, Maaloe O, Neidhardt FC. 1983. Growth of the Bacterial Cell. Sinauer Associates Incorporated.

Malik, VS. 1980. Microbial secondary metabolism. Cell Press 5(3): 1-7.

Procopio RE, Silva IR, Martins MK, Azevedo JL, Araujo JM. 2012. Antibiotics produced by *Streptomyces*. Brazilian Journal of Infectious Diseases 16(5): 466-471.

Sarkar P, Yarlagadda V, Ghosh C, Haldar J. 2017. A review on cell wall synthesis inhibitors with an emphasis on glycopeptide antibiotics. MedChemComm 8(3), 516-533.

Silhavy TJ, Kahne D, Walker S. 2010. The Bacterial Cell Envelope. Cold Spring Harbor Perspectives in Biology 2(5), DOI: 10.1101/cshperspect.a000414.

Xu Z, Wang Y, Chater KF, Ou HY, Xu H, Deng Z, Tao M. 2016. Large-Scale Transposition Mutagenesis of *Streptomyces coelicolor* Identifies Hundreds of Genes Influencing Antibiotic Biosynthesis. American Society for Microbiology 83(6), 1-16.